Astron. Astrophys. 357, 206–218 (2000)

ASTRONOMY AND ASTROPHYSICS

A multi-wavelength study of pre-main sequence stars in the Taurus-Auriga star-forming region

E.W. Guenther[1], B. Stelzer[2], R. Neuhäuser[2], T.C. Hillwig[3], R.H. Durisen[3], K.M. Menten[4], R. Greimel[5,7], H. Barwig[6], J. Englhauser[2], and R.M. Robb[7]

[1] Thüringer Landessternwarte Tautenburg, Karl-Schwarzschild-Observatorium, Sternwarte 5, 07778 Tautenburg, Germany
[2] Max-Planck-Institut für Extraterrestrische Physik, Giessenbachstrasse 1, 85740 Garching, Germany
[3] Department of Astronomy, SW319, Indiana University, Bloomington, Indiana 47405, USA
[4] Max-Planck-Institut für Radioastronomie, Auf dem Hügel 69, 53121 Bonn, Germany
[5] Isaac Newton Group, Astronomy Division, Apartado de Correos, 321, 38780 Santa Cruz de La Palma, Canary Islands, Spain
[6] Universitäts-Sternwarte München, Scheinerstrasse 1, 81679 München, Germany
[7] Department of Physics and Astronomy, University of Victoria, P.O. Box 3055, Victoria, BC, V8W 3P6, Canada

Received 9 December 1999 / Accepted 25 February 2000

Abstract. Although many lowmass pre-main sequence stars are strong X-ray sources, the origin of the X-ray emission is not well known. Since these objects are variable at all frequencies, simultaneous observations in X-rays and in other wavelengths are able to constrain the properties of the X-ray emitting regions. In this paper, we report quasi-simultaneous observations in X-rays, the optical, and the radio regime for classical and weak-line T Tauri stars from the Taurus-Auriga star-forming region. We find that all detected T Tauri stars show significant night-to-night variations of the X-ray emission. For three of the stars, FM Tau and CW Tau, both classical T Tauri stars, and V773 Tau, a weak-line T Tauri star, the variations are especially large. From observations taken simultaneously, we also find that there is some correspondence between the strength of Hα and the X-ray brightness in V773 Tau. The lack of a strong correlation leads us to conclude that the X-ray emission of V773 Tau is not a superposition of flares. However, we suggest that a weak correlation occurs because chromospherically active regions and regions of strong X-ray emission are generally related. V773 Tau was detected at 8.46 GHz as a weakly circularly polarised but highly variable source. We also find that the X-ray emission and the equivalent width of Hα remained unchanged, while large variations of the flux density in the radio regime were observed. This clearly indicates that the emitting regions are different. Using optical spectroscopy we detected a flare in Hα and event which showed a flare-like light-curve of the continuum brightness in FM Tau. However, ROSAT did not observe the field at the times of these flares. Nevertheless, an interesting X-ray event was observed in V773 Tau, during which the flux increased for about 8 hours and then decreased back to the same level in 5 hours. We interpret this as a long-duration event similar to those seen on the sun and other active stars. In the course of the observations, we discovered a new weak-line T Tauri star, GSC-1839-5674. Results are also presented for several other stars in the ROSAT field.

Key words: stars: flare – stars: formation – stars: late-type – stars: pre-main sequence – Galaxy: open clusters and associations: general

Send offprint requests to: E.W. Guenther
Correspondence to: Thüringer Landessternwarte, 07778 Tautenburg, Germany

1. Introduction

Classical T Tauri stars (hereafter cTTSs) are now recognized as pre-main sequence stars accreting material from an extended circumstellar disk (Appenzeller & Mundt 1989). Weak-line T Tauri stars (hereafter wTTSs) are similar to the classical ones but lack massive disks and have little or no accretion. Research in the past ten years has made clear the importance of strong magnetic fields in these stars. A sign of this activity is the generally large brightness of these objects in the X-ray regime. Since the launch of the Einstein X-ray satellite, it is well known that both types of T Tauri stars are strong, variable X-ray sources. The X-ray brightness of these stars is often more than one thousand times stronger than the emission from the solar corona. In fact, most of the wTTSs that we know today were detected in X-ray surveys carried out by ROSAT. The strong X-ray emission of young stars is not only important as indirect evidence for the presence of strong magnetic fields in these stars, but the X-rays may also by important for the ionisation of the circumstellar disk (Glassgold et al. 1997a; Glassgold et al. 1997b; Igea & Glassgold 1999). Despite the presumably great importance of X-ray emission for T Tauri stars, its origin is still not well understood. In this paper, we undertake quasi-simultaneous observations of T Tauri stars in the X-rays, the optical, and the radio regime. In this way, we try to shed more light on the origin of the X-rays and the structure of the emitting region.

One possibility, especially for the wTTSs, is that the X-ray emission arises in a hot corona, like on the sun, only much larger.

The hot corona picture seems quite attractive, because the relatively rapid rotation of T Tauri stars compared with the sun may lead to the creation of a super-corona. Still, however, it is an open question whether an α-Ω dynamo operates in young stars. For solar-type stars, where we know that the X-ray emission comes from a hot corona, there is a tight correlation between the rotational velocity of the star and the X-ray emission. This correlation is thought to be due to the correlation between the differential rotation and the magnetic field strength in an α-Ω dynamo. Neuhäuser et al. (1997) in fact found a correlation between the X-ray emission and the rotational velocity for young stars in the Taurus-Auriga region. However, no such correlation was found for stars in the Chameleon I star-forming region (Feigelson et al. 1993).

The wTTSs also show clear signs of an active chromosphere, as the emission feature in the core of the Ca II H,K lines is visible for most of these stars. Often, this feature is even stronger than in solar plage regions. In many wTTSs, Hα is also in emission. If the hot corona model is correct, we expect to observe some correlation between the chromospheric emission and the X-ray emission from the corona, but that correlation would not be one-to-one, like on the sun. By studying the relation between the chromospheric features and the emission of the corona in X-rays, it is thus possible to shed more light on the origin of the X-rays.

The cTTSs, by definition, have very strong emission lines, notably Hα. It is now well accepted that these features can certainly not be attributed to chromospheric activity but are usually interpreted as due to magnetically funneled accretion from the inner part of the accretion disk. The funneled matter falls freely along the magnetic field lines towards the star. The shape of the higher Balmer lines and of hydrogen emission lines in the infrared can in fact be reproduced if an origin in the funnel flow is assumed (Muzerolle et al. 1998). However, since the optical thickness of Hα is much larger than that of higher Balmer lines or the hydrogen lines in the infrared an inverse P-Cygni profile, indicating infall, is only extremely rarely seen in Hα (Alcalá et al. 1993). Observations by Hessman & Guenther (1997) show that the flux of the emission lines and the strength of the veiling continuum are well correlated, indicating that the emitting regions are either identical or physically linked. The magnetic accretion model has recently gained further support as the required strong fields have in fact been detected in a few cases (Guenther et al. 1999). In cTTSs, there are in principle two possibilities for the origin of the X-ray emission: the X-rays may originate from a hot, extended corona, as in the wTTSs (Neuhäuser et al. 1997 and the references therein), or the X-rays may be generated in the accretion shock at the base of the funneled flow (Gullbring 1994; Lamzin et al. 1996). Since the velocity of the infalling matter may reach velocities of up to 300 $\mathrm{km\,s^{-1}}$, soft X-rays are generated in the accretion shock. Although the free path length of such radiation in the dense circumstellar environment of a cTTS is expected to be small, it cannot be ruled out that some of the observed X-ray emission is generated there. In this model, the X-rays would then come from the shock, and the emission lines would be the funneled flow. However, without extra assumptions, it is not easy to understand where the X-ray flares come from in this model.

This model has some resemblance to that for AM Her systems. In an AM Her system, the hard thermal X-ray radiation produced behind the shock locally heats the white dwarf atmosphere which then radiates as a blackbody with a temperature of a few 10^5 K. The accreted gas in an AM Her system is observed as strongly polarised optical/IR emission. Since observation of AM Her systems do not show a correlation between the X-ray emission and the optical emission (Crosa et al. 1981; Paerels et al. 1994), we would expect the same for cTTSs if the X-ray emission comes from the accretion shock. Simultaneous observations in X-rays and in the optical regime can thus also test the magnetically funneled accretion scenario.

As pointed out before, the X-ray emission of young stars is highly variable. At least part of the X-ray emission is due to flares. Strong X-ray flares have been reported for a number of T Tauri stars (Preibisch et al. 1995, Preibisch et al. 1993). Since flares are known to be produced on the sun by the rapid release of magnetic energy, such events can be taken as evidence that magnetic fields are present on these stars. The size of the X-ray flares of young stars are enormous, often hundreds of times larger than the largest flares on the sun. Recent observations have shown that similar events can also be observed in the optical regime (Guenther & Ball 1999). An interesting aspect of flares is that the coronae of magnetically active solar-type stars might actually be heated by flares (Güdel 1997).

Flares are not only important as indirect evidence for the presence of magnetic fields in young stars but might also be important for ionising the circumstellar disk. Flares lead to an increased X-ray flux, harden the X-ray spectrum, and increase the flux of high-energy particles (Glassgold et al. 1997a; Tsuboi et al. 1998). Although flare activity declines with stellar age, flares could also be important in later stages of evolution, because the EUV and X-ray emission of the young sun might have been important for the formation of planetary ionospheres (Canuto et al. 1982; Canuto et al. 1983; Güdel et al. 1997). Simultaneous optical and X-ray observations of solar flares show that the light curves of Hβ and soft X-rays (0.25–4.0 keV) are almost identical, implying that Balmer-lines are probably produced during a flare by reprocessing of the soft X-ray radiation (Johns-Krull et al. 1997). The same close relation between X-ray emission and Hα is also observed in flares on RS CVn and BY Dra stars (Doyle et al. 1988). Thus, if the Hα-line and X-ray emission were just a superposition of solar-like flares, we would expect a very strong correlation between them.

Simultaneous observations of flares in the optical and in the X-ray regime are required in order to determine whether the optical events are really the counterparts of the X-ray events. Thus multi-frequency observations of flares in young stars are a very powerful tool and should be undertaken despite the difficulty. The only attempt to observe a cTTS (BP Tau) simultaneously in the optical and in X-rays was unsuccessful, because no optical data were obtained at the moment when an X-ray flare occurred (Gullbring et al. 1997). A small optical variation had no counterpart in the X-rays. In this paper, we report on another attempt

to observe a number of cTTSs and wTTSs simultaneously in the optical and in the X-ray regime. Although we too failed to capture a flare simultaneously in the X-rays and other wavelengths, we do have multi-wavelength data on the activity of these stars over a time interval of several days.

2. Observations and data-reduction

2.1. The targets

For this project we selected the small dark cloud Barnard 209 which is part of the Taurus-Auriga star-forming complex. This region contains a number of very active cTTSs and wTTSs. The prime targets in the field of view are the wTTS V773 Tau and the cTTSs FM Tau, CW Tau and Briceño 1. The properties of these objects will be described together with the data in Sect. 4.

2.2. Optical spectroscopy with CAFOS

Using the faint object spectrograph CAFOS of the 2.2m telescope of the German Spanish Astronomical Centre (DSAZ) on Calar Alto, we have observed the T Tauri stars V773 Tau, CW Tau, FM Tau and Briceño 1. Since we used a slit mask, all four stars were observed simultaneously. The exposure times were always 200s, resulting in a cycle frequency of about 300s. The spectra were obtained using the "BLUE" grism, which gives a dispersion of 100 Å mm^{-1}, corresponding to 1.97 Å pixel^{-1} for the SITE 2kx2k chip used. The spectra cover the wavelength region between about 3200 Å and 6330 Å. Standard IRAF routines were used to subtract bias, flat-field, remove the scattered light, subtract the sky background, and extract and wavelength calibrate the spectra. The different parts of the spectra were relative flux calibrated using $\mathrm{BD} + 28^{\circ}4211$ and its tabulated fluxes.

2.3. Optical spectroscopy with Hydra

We used the fiber-fed spectrograph HYDRA on the 3.5m WIYN telescope [1] at Kitt Peak National Observatory, to obtain low-resolution spectra which cover the wavelength region between about 6090 Å and 7030 Å. The dispersion was 0.45 Å pixel^{-1} with the Tektronix 2k CCD chip. Exposure times between 600 and 900s were used, depending on the sky conditions. Because HYDRA permits observations of many objects simultaneously, in addition to V773 Tau, FM Tau, HBC 366 (=Anon 1), and CW Tau, we also observed Briceño 1, Briceño 2, FN Tau, FO Tau, GSC-1839-5674, GSC-1839-2008, IRAS04113+2758, LkCa 1, and LkCa 2. Standard IRAF routines were again used to subtract bias, flat-field, remove the scattered light, subtract the sky background and extract and wavelength calibrate the spectra.

[1] The WIYN telescope is maintained and operated by a consortium whose member institutions are University of Wisconsin, Indiana University, Yale University, and the National Optical Astronomy Observatories.

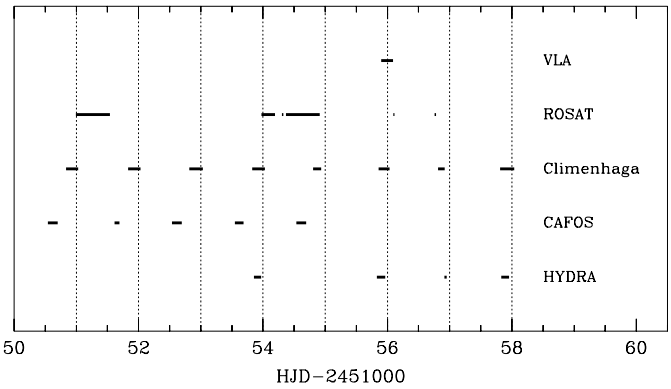

Fig. 1. Journal of the observations. The X-ray observations were carried out with ROSAT, optical spectroscopy was carried out with CAFOS and HYDRA, and photometric observations were carried out at Climenhaga Observatory. HJD is the Heliocentric Julian Date.

2.4. Optical photometry

Using the robotic 0.5m telescope of the University of Victoria (Canada) at Climenhaga Observatory, we obtained CCD images of a region centred on V773 Tau in the Cousin R-band. The size of the region was 8.2×5.5 arc-minutes and thus covers V773 Tau, FM Tau, and CW Tau. While all the stars in the field were variable, the data still can be used to obtain relative photometry between the T Tauri stars. Data reduction was performed using the IRAF *apphot* package using a mask with a 7.7″ radius. The typical cycle time was three minutes. The system has proven extremely stable and the data were reduced in a fashion identical with Robb et al. (1997).

We also attempted to observe the V773 Tau field using the 80cm Cassegrain Telescope of the Universitäts-Sternwarte München at Wendelstein Observatory. Unfortunately, it never cleared up during the whole observing run.

2.5. X-ray observations

We also obtained ROSAT HRI observations pointed towards V773 Tau. Due to problems with the attitude control during part of these X-ray observations, we were forced to ignore all times with unstable attitude for the major part of our analysis. The overlap between optical and X-ray observations is significantly reduced after the unstable time intervals have been eliminated from the data set (see Fig. 1). The 'good' data intervals are summarised in Table 1. Since we are interested in the time development of the count rates, the six observations from Table 1 have not been merged to search for faint detections.

Source detection was performed with combined local and map source detection algorithms based on the maximum likelihood method as implemented in EXSAS (Zimmermann et al. 1995). For most of the observation intervals given in Table 1, we found a systematic misplacement between X-ray sources and optical positions of the stars. Such discrepancies are the result of limitations in the satellite's pointing accuracy and the respective X-ray images must be 'boresight corrected'. This is usually done by comparison of the optical and X-ray positions

Table 1. *ROSAT* HRI observations centred on V773 Tau

ROR	$T_{\rm start}$ [date,UT]	$T_{\rm stop}$ [date,UT]	Exposure [sec]
202805h (A)	25-08-98 11:50	26-08-98 00:59	14621
202808h (A)	28-08-98 11:25	28-08-98 16:38	5239
202808h (B)	28-08-98 19:15	28-08-98 19:49	1820
202809h (A)	28-08-98 20:51	29-08-98 09:55	16200
202809h (B)	30-08-98 14:14	30-08-98 14:40	1526
202805h (B)	31-08-98 06:09	31-08-98 06:41	1842

Note: Only good data intervals were used

of bright X-ray sources. In our case, we individually correct the positioning of each HRI observation using the mean offset from 3 stars in each field. The nominal positional accuracy of the ROSAT HRI is 25″. However, as mentioned above during the last ROSAT HRI observations the pointing accuracy was much worse. We therefore allow for a maximum displacement between optical and X-ray position of 25 arcsec. For the extraction of the photons the 99% quantile of the point spread function at 1 keV was used.

2.6. VLA observations

We observed V773 Tau with the National Radio Astronomy Observatory (NRAO)[2] Very Large Array (VLA) on 1998 August 30 when the array was in its B-configuration. Right and left circularly polarised (RCP and LCP) intensity was observed, each with a bandwidth of 100 MHz centred at a frequency of 8.46 GHz. We took a total of 4 "scans" in ≈ 1.5 hour intervals; each scan had a duration of ≈ 4 min (see Table 3 for exact times) and was sandwiched between observations of the extragalactic radio source 0414+343, which were made to provide phase calibration. The flux density scale was established by observing 3C147. The data were edited, calibrated, and imaged following standard procedures and using the AIPS software package. We estimate that the flux density scale is accurate to 5%.

3. Results

3.1. General remarks on the X-ray data

The X-ray count rates and luminosities are summarised in Table 2 for all detected and undetected objects for each observation (see Table 1). Only two T Tauri stars, V773 Tau and HBC 366, have been detected in all 6 observation intervals. However, the images on ROR 202805h (ROR=ROSAT observation request number) were extremely elongated. In order to measure the flux of V773 Tau, we would have to use quite a large aperture, which would have included the X-ray flux of FM Tau too. The measurements of the X-ray flux are shown in Table 2. Some of our T Tauri stars are not detected in any of the pointings. In the case of non-detections, we give upper limits.

[2] NRAO is operated by Associated Universities, Inc. under a cooperative agreement with the National Science Foundation.

In the following, we will describe the X-ray data together with the optical data for our prime targets – the wTTS V773 Tau and the cTTSs Briceño 1, FM Tau and CW Tau. However, Briceño 1 has not been detected by ROSAT at all. FM Tau has been detected in four of the six RORs, and CW Tau in only one. HYDRA and ROSAT observations of the other objects in the field of view will be described at the end of this section.

3.2. The wTTSs triple star V773 Tau

3.2.1. The object V773 Tau

The brightest object in soft X-rays in the observed region is the wTTS V773 Tau (=HD 283447). This object is a peculiar triple star. It consists of a wide optical binary with a separation of about 0.07 to 0.11 arcsec (corresponding 10 to 15 AU) (Ghez et al. 1995). The brighter component of the binary is a double-line spectroscopic binary with a period of 51.075 days (Welty 1995). The projected distance $(a_1 + a_2)\, sin\, i$ of the close binary is 0.34 AU. The minimum masses for this pair are 1.17 ± 0.11 and $0.89 \pm 0.09\ \mathrm{M}_\odot$ (Welty 1995). Although V773 Tau is a pre-main sequence object, the system resembles in many respects an RS CVn star. V773 Tau is highly variable and is a very luminous nonthermal radio source (O'Neal et al. 1990; Phillips et al. 1991; Dutrey et al. 1996; Phillips et al. 1996). VLBI observations show two components with a separation of 0.3 AU, which is most likely the inner binary system. Radial velocity variations with an amplitude of $3\,\mathrm{km\,s^{-1}}$ and with a period of about three days were detected by means of optical spectroscopy in both components (Welty 1995). This three day period must be the rotation period of the stars, as it corresponds well with the period of V-band variations of 3.43 days (Rydgren & Vrba 1983). The rotation period of both components must be around three days and is thus significantly different from the orbital period. The radial velocity variations also indicate the presence of large surface inhomogeneities (i.e. spots).

V773 Tau is also well known for its strong flare activity. An enormous X-ray flare was detected by the ASCA satellite and reached a temperature of 10^8 K. A simple cooling-loop model of such a flare gives electron densities that are similar to those of solar flares but requires a loop size of about one stellar radius (Tsuboi et al. 1998; Skinner et al. 1997). The system has also been studied in a coordinated campaign in which the object was simultaneously observed for several hours at X-ray, ultraviolet, optical, and radio wavelengths (Feigelson et al. 1994). During this observing period, the radio luminosity decreased by a factor of four, while no change was seen in the X-ray flux nor in the strength of the optical emission lines. This indicates that the region of gyrosynchrotron emission is presumably different from the optical and the X-ray emitting regions.

3.2.2. The X-ray data

As expected, V773 Tau is the brightest X-ray source in the HRI field of view. V773 Tau is sufficiently bright to make use of *all* observing times (except 202805h), i.e. we also used the data in-

Table 2. X-ray data of all TTSs in the HRI field. Count rates or upper limits are listed for each of the observation intervals from Table 1. Columns 3, 4,and 5 give the off-axis angle of the X-ray source, the offset between optical and X-ray position before boresight corrections, and the maximum likelihood of the detection, respectively.

Designation	Count Rate $[10^{-3}\,\mathrm{cts/s}]$	off-axis [arcmin]	Δ [arcsec]	ML
202805h (A)				
LkCa 1	< 2.21	17.50	-	
HBC 366	17.88±1.25	13.79	3.0	381.7
V773 Tau	93.71±2.60	3.32	5.1	2627.8
FM Tau	0.81±0.27	3.41	10.4	13.5
FN Tau	< 0.93	16.49	-	
CW Tau	< 0.07	2.87	-	
Briceño 1	< 0.24	6.38	-	
IRAS 04113+2758	2.47±0.45	6.25	3.9	52.2
IRAS 04114+2757	0.65±0.26	7.04	6.6	7.5
HD 26709	1.95±0.57	14.48	5.6	10.0
LkCa 3	< 0.21	19.98	-	
FO Tau	< 0.32	5.19	-	
GSC-1839-5674	3.38±0.54	8.38	2.6	49.4
Briceño 2	0.96±0.32	9.17	7.6	11.7
202808h (A)				
LkCa 1	< 0.10	18.18	-	
HBC 366	13.41±1.89	14.50	6.0	83.4
1419.6				
V773 Tau	101.21±4.50	3.85	7.8	1419.6
FM Tau	0.99±0.49	3.85	4.8	7.9
FN Tau	< 1.18	16.46	-	
CW Tau	< 0.13	3.27	-	
Briceño 1	< 0.06	6.64	-	
IRAS 04113+2758	1.43±0.58	6.28	11.9	9.5
IRAS 04114+2757	< 0.57	7.00	-	
HD 26709	4.71±1.25	14.51	3.5	15.4
LkCa 3	< 0.57	19.88	-	
FO Tau	< 0.03	4.35	-	
GSC-1839-5674	4.90±1.09	7.88	5.2	26.0
Briceño 2	1.54±0.63	8.44	3.6	8.5
202808h (B)				
LkCa 1	< 0.41	18.10	-	
HBC 366	9.87±2.69	14.38	19.0	23.3
31.3				
V773 Tau	126.29±8.53	3.70	23.0	625.8
FM Tau	< 0.34	3.80	-	
FN Tau	< 2.32	16.83	-	
CW Tau	< 0.41	2.95	-	
Briceño 1	< 0.38	6.17	-	
IRAS 04114+2758	< 0.35	5.85	-	
IRAS 04114+2757	< 1.01	6.60	-	
HD 26709	< 2.76	14.09	-	
LkCa 3	< 2.35	19.53	-	
FO Tau	< 0.45	4.70	-	
GSC-1839-5674	< 1.43	7.74	-	
Briceño 2	< 1.64	8.55	-	

Designation	Count Rate $[10^{-3}\,\mathrm{cts/s}]$	off-axis [arcmin]	Δ [arcsec]	ML
202809h (A)				
LkCa 1	< 0.92	18.23	-	
HBC 366	13.14±1.06	14.53	15.1	244.0
V773 Tau	102.92±2.58	3.87	15.6	3949.9
FM Tau	0.88±0.27	3.93	18.6	18.7
FN Tau	< 1.34	16.71	-	
CW Tau	0.45±0.20	3.18	16.5	7.7
Briceño 1	< 0.14	6.41	-	
IRAS 04113+2758	1.10±0.31	6.05	19.6	13.1
IRAS 04114+2757	< 0.20	6.78	-	
HD 26709	< 0.91	14.26	-	
LkCa 3	< 0.25	19.65	-	
FO Tau	< 0.001	4.46	-	
GSC-1839-5674	5.35±0.63	7.74	18.4	117.6
Briceño 2	1.07±0.32	8.41	14.5	13.6
202809h (B)				
LkCa 1	< 3.31	18.44	-	
HBC 366	19.46±4.08	14.79	3.9	38.8
V773 Tau	58.49±6.35	4.11	3.8	202.6
FM Tau	< 1.63	4.07	-	
FN Tau	< 2.33	16.37	-	
CW Tau	< 0.12	3.46	-	
Briceño 1	< 0.67	6.77	-	
IRAS 04113+2758	< 1.53	6.31	-	
IRAS 04114+2757	< 0.55	7.01	-	
HD 26709	< 1.92	14.56	-	
GSC-1839-5674	4.93±2.01	7.72	4.0	9.3
FO Tau	< 2.08	3.96	-	
Briceño 2	< 0.78	8.17	-	
202805h (B)				
LkCa 1	< 3.00	18.41	-	
HBC 366	15.00±3.24	14.82	5.1	40.1
V773 Tau	55.80±5.67	4.31	2.3	205.2
FM Tau	3.76±1.47	4.19	5.4	18.9
FN Tau	< 3.28	15.90	-	
CW Tau	< 0.36	3.82	-	
Briceño 1	< 1.25	7.32	-	
IRAS 04113+2758	< 0.34	6.87	-	
IRAS 04114+2757	< 1.35	7.56	-	
HD 26709	< 1.80	15.10	-	
FO Tau	< 0.35	3.81	-	
GSC-1839-5674	4.24±1.65	8.07	6.4	11.9
Briceño 2	2.94±1.37	8.27	3.4	9.1

tervals excluded due to the attitude instability. In order to correct for smearing of the source by the inaccurate pointing position, we separated all available data into individual satellite orbits. For each of the resulting time intervals, we created an X-ray image on which we identify V773 Tau. We subsequently defined a rectangular box around the source within which we determined the number of counts. The size of the box is optimised so that as many photons as possible are included while an overlap with

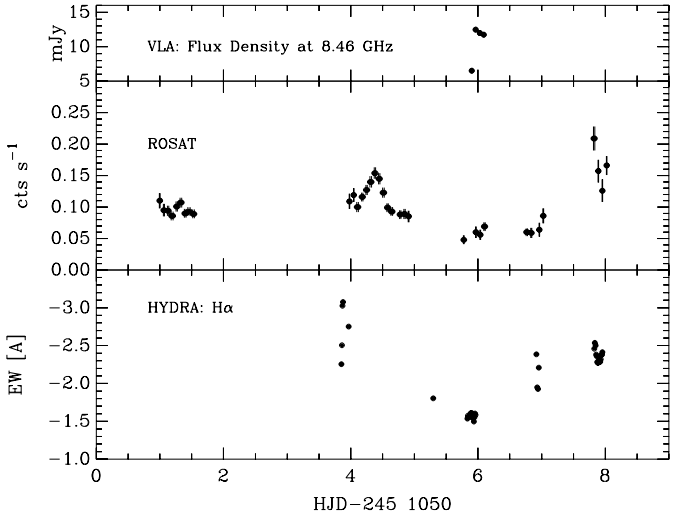

Fig. 2. The upper panel shows the flux density at 8.46 GHz of V773 Tau, the middle panel ROSAT count rate, and the lowest panel the equivalent width of Hα. An enlarged version showing the event on HJD 245 1054 is seen in Fig. 3.

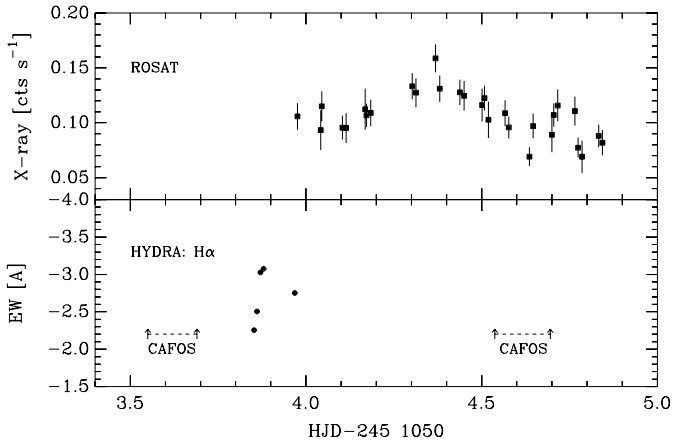

Fig. 3. Enlarged version of Fig. 2. Shown is the event on HJD 245 1054 in more detail. The upper panel are the ROSAT X-ray data, the lower the equivalent width measured in Hα using HYDRA. The errors of the latter measurements are too small to be seen. Also indicated are the times when the object was observed with CAFOS. On this day, the X-ray brightness of the object increased steadily for 8 hours, and then declined again for five hours. Shortly before the slow X-ray event happened, we observed a rapid increase and slow decline of the equivalent width of Hα.

adjacent (detected or undetected) T Tauri stars is minimised. A box of the same area is placed at a source-free region to extract the background. We then divided both numbers by the exposure time and obtained an estimate for the mean count rate during the respective satellite orbit. A rectangular shape for the extraction region is required, because even after the selection into separate satellite orbits the source appears to be elongated.

All other stars are not bright enough to be identified by visual inspection of the X-ray images. Therefore, we could not apply our box method. We have instead generated X-ray light-curves of the 'good' time intervals for all detections using 400s integration time.

3.2.3. Variability in X-rays and in the optical

Fig. 2 shows the ROSAT count rate of V773 Tau, together with the equivalent width of Hα and the radio data. The X-ray brightness is highly variable. The night-to-night variations are often as large as a factor of two (see also Table 2). The most interesting feature is the X-ray event on HJD 245 1054 which is shown in more detail in Fig. 3 (HJD is the Heliocentric Julian Date). On this day the X-ray flux increased steadily for about 8 hours and then declined for 5 hours. At the peak-luminosity, the X-ray flux of V773 Tau is $40 \pm 16\%$ higher than before the event. Also shown in Fig. 3 is the equivalent width of Hα. The optical data was taken shortly before the X-ray event. Seen is a relatively rapid increase and slow decay of the equivalent width, possibly a small flare. In the CAFOS spectra, Hβ is generally filled in and thus not seen. The most pronounced line in this spectral region thus is the (unresolved) NaD doublet. Fig. 4 shows a section of the two CAFOS spectra taken at the times that are marked in Fig. 3. No obvious differences between the two spectra could be found.

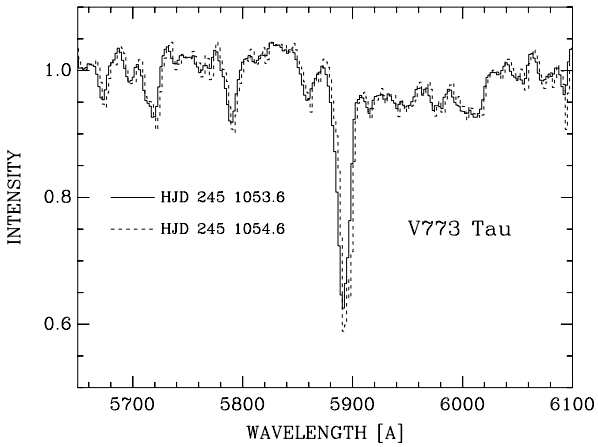

Fig. 4. Part of the two CAFOS spectra of V773 Tau taken at the times indicated in Fig. 3. The prominent absorption line in the middle are the two unresolved NaD lines. We do not find any obvious differences between the two spectra.

Significant variability in Hα (taken with the WIYN) was also observed on HJD 245 1057. However, only four spectra were taken that night, and these spectra were all taken within one hour. This time ROSAT observed the field simultaneously to the optical data. During the six hours in which ROSAT observed the field, a steady increase of the X-ray emission was observed. Towards the end of HJD 245 1057 V773 Tau was quite bright in X-rays, and the X-ray brightness was variable. On the same day, Hα was quite strong but showed only very little signs of variability.

In Fig. 5 we plotted the equivalent width of Hα against the X-ray flux for all times at which ROSAT observed the object simultaneously with HYDRA. There seems to be a trend that when

Table 3. VLA Results: 8.46 GHz flux densities

HJD-2451000	UT Time on 1998 Aug 30	Flux Density at 8.46 GHz $S(I)$ (mJy)	$S(V)$ (mJy)
55.9001-55.9032	09:36:00–09:40:30	6.51(0.08)	0.52(0.06)
55.9626-55.9656	11:06:00–11:10:20	12.46(0.05)	0.72(0.06)
56.0286-56.0313	12:41:00–12:45:00	11.98(0.06)	0.98(0.07)
56.0874-56.0903	14:05:40–14:09:50	11.76(0.10)	0.97(0.07)

Note: $S(I)$ and $S(V)$ are the total and circularly polarised flux densities, respectively (I and V are the Stokes I and V parameters). Their 1σ uncertainties are listed in parentheses.

the object gets brighter in X-rays, the Hα equivalent width becomes larger. The correlation coefficient is 0.64. If we leave out the data from the end of HJD 245 1057, the trend still remains. Formally the correlation becomes somewhat larger (0.92). Thus there seems to be some relation between the X-ray brightness and the strength of Hα, but it is certainly not a one-to-one correlation.

3.3. VLA results

V773 Tau has been observed several times with the VLA since its first radio detection by Kutner et al. (1986), who measured a flux density of 3.6 mJy at a wavelength of 6 cm.

We imaged each of the four 4 min-duration scans separately and found that the source is variable on a timescale of hours and weakly circularly polarised (see Table 3). To search for variability on smaller timescales, we determined the flux densities for 1 min segments of data and did not find significant variability on a timescale of minutes. Interestingly, despite the large changes of the flux density at 3.5 cm, the X-ray flux and the equivalent width in Hα did not change significantly during this time (Fig. 2). This implies that the regions from which the X-ray radiation, and the emission line flux originate can not be the same as the radio emitting region.

White et al. (1992) observed V773 Tau using the VLA at 5 GHz and found, like us, the emission to be weakly polarised (we find the degrees of polarisation to be varying between 0.12 and 1.59) and variable on scales of hours but not on scales of minutes.

3.4. The cTTS FM Tau

3.4.1. The object FM Tau and night-to-night variations

FM Tau is a cTTS that is known to show some flare activity in the optical regime (Guenther & Ball 1999). It is also relatively bright in X-rays and has been detected in four RORs. However, FM Tau is not bright enough to allow us to do the same analysis as for V773 Tau, and thus only nightly averages of the X-ray brightness are derived. Fig. 6 shows the variations of equivalent width in Hα and Hβ, together with the variable X-ray emission. From HJD 2451054 to HJD 2451056 the X-ray flux increased by a factor of four (see also Table 2). The curve of the equivalent width in Hβ shows generally slow and smooth variations. Unfortunately, the overlap with good ROSAT data is too small to conclude anything on the relation between X-ray emission and strength of the emission lines. It can only be stated that comparatively large variations of the X-ray brightness and the strength of the Balmer lines were observed.

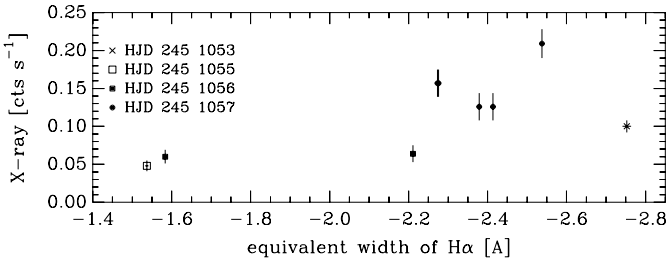

Fig. 5. The X-ray brightness plotted against the equivalent width of Hα for V773 Tau. This plot uses only data when the X-rays and optical were observed simultaneously. This data indicates that there is a trend that, with increasing equivalent width of Hα, the object also tends to brighten in X-rays.

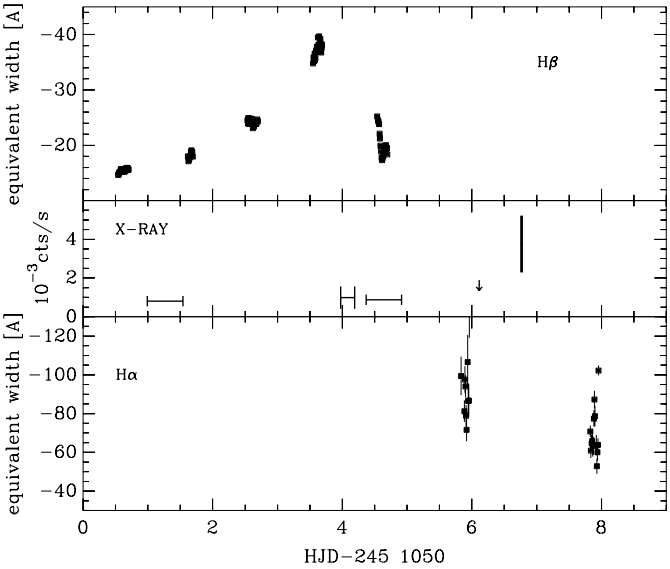

Fig. 6. FM Tau: The upper panel shows the equivalent width of Hβ, and the lower panel the equivalent width of Hα for FM Tau. The middle panel is the ROSAT count rate. X-ray detections are shown as full line with the errors indicates at the beginning and at the end of the observations. The upper limit is indicated as an arrow pointing downwards. The event which is shown in Fig. 8 was on 245 1058.

3.4.2. A flare-like event observed in the continuum

As described in Sect. 3.1.3, we took CCD images of the field containing V773 Tau, FM Tau, and CW Tau with the Climenhaga Observatory 0.5m telescope. Since all three stars are variable, and no other stars were in the field, it is not possible to derive light-curves for the stars individually. The lowest panel in Fig. 7 shows the difference between Cousin R-magnitudes of CW Tau and V773 Tau on HJD 245 1052. During the whole night, this difference stayed almost constant. Since it is highly

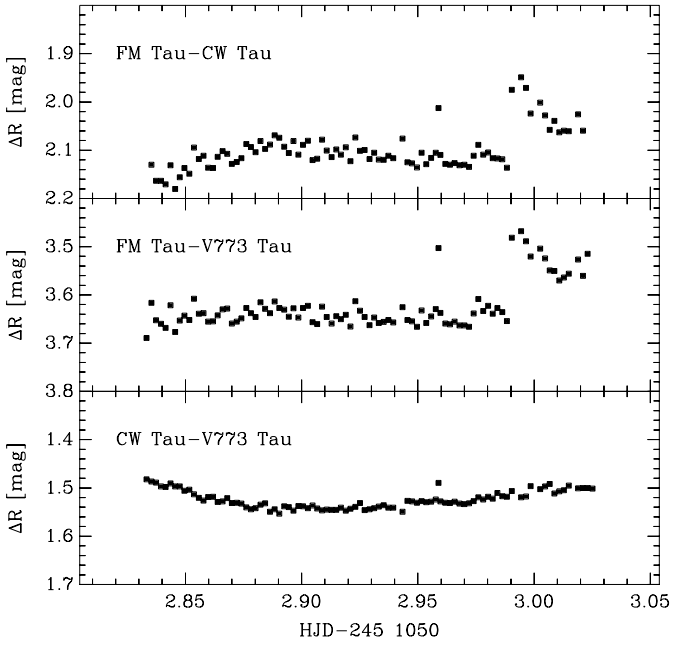

Fig. 7. The figure shows differences in brightness of V773 Tau, CW Tau, and FM Tau in the Cousin R-band. Although all three stars are in principle variable, we find that on this particular night the brightness difference between V773 Tau and CW Tau remained quite constant. We thus conclude that the peak which is seen in the middle and upper panel is due to an increase of the brightness of FM Tau. Additionally, we conclude that the brightness of FM Tau increased within three minutes by 0.169 ± 0.019. This increase was then followed by a slow decrease of brightness. The event thus seems to be a continuum flare on FM Tau.

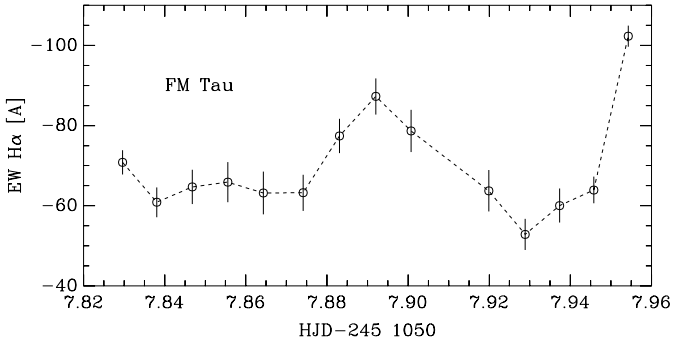

Fig. 8. Variations of the Hα equivalent width of FM Tau. A flare-like event can be seen.

unlikely that both stars changed the brightness in the same way, we assume that the brightness of both stars did not change during this night. Since the difference in brightness between FM Tau and V773 Tau and between FM Tau and CW Tau both show a peak of the same height at the end of the night, it is reasonable to assume that this peak is caused by a change in the brightness of FM Tau. If CW Tau and V773 Tau remained constant, this peak would indicate that FM Tau got brighter. For the difference in brightness between FM Tau and V773 Tau, we find 3.644 ± 0.017 mag before the event and 3.475 ± 0.007 mag at the peak. For FM Tau and CW Tau, we find 2.114 ± 0.015 mag

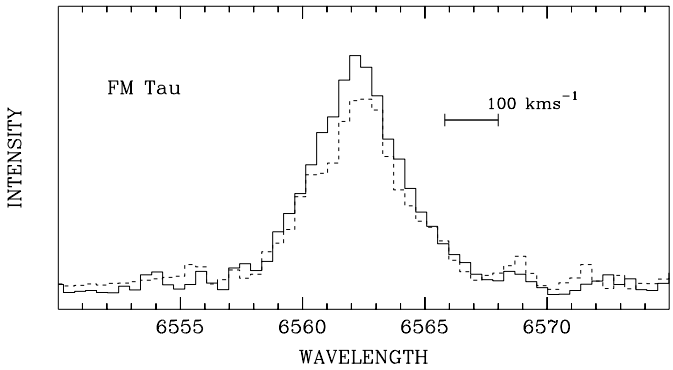

Fig. 9. Profiles of the Hα line before (dashed, HJD 245 1057.82959 to 245 1057.87416) and during the event (HJD 245 1057.89206) shown in Fig. 8. The largest difference between the two line-profiles is in the blue-part of the spectrum.

before, and 1.975 ± 0.011 mag at the peak. From the two datasets, we thus conclude that the brightness of FM Tau increased by 0.169 ± 0.018 and 0.169 ± 0.019 mag in the R-band, respectively. The increase in brightness apparently took less than three minutes, our time-resolution. The field was then observed for another 45 minutes, until the observations were stopped because of the dawn. During this time, the brightness of FM Tau decreased. The last few data-points seem to have been affected by the increase of the sky-brightness. If we ignore these points, we estimate a decline-time of about an hour. The light-curve of the event was thus much like that of a flare.

3.4.3. A flare in Hα on FM Tau

An interesting feature of the Hα-curve is the event on HJD 245 1058 which is shown in more detail in Fig. 8. The errorbars were calculated from the photon noise of FM Tau, the read-out noise of the CCD camera, and also the noise that was introduced by the subtraction of the sky background. The event lasted for about half an hour, and the rise time was shorter than the decay time. Fig. 9 shows the profiles of the Hα line before (dashed) and during the events shown in Fig. 8. We note a small difference between the shape of the line-profiles in the Hα line: The increase in flux of the Hα line is stronger in the blue wing than in the red. At the end of the night, the equivalent width of FM Tau went up again, perhaps the beginning of a second, bigger event. Although the observed event is relatively small, it does have the typical properties of flares on a cTTS. Multiple events, as observed here, are also quite typical for flares. Observing a flare on FM Tau is not unusual, as optical flares have been detected before on this star (Guenther & Ball 1999). However, this time we observed the event in Hα, not in the higher Balmer lines, as previously. Fig. 10 shows the difference between Cousin R-magnitudes of V773 Tau, CW Tau and FM Tau on HJD 245 1057 as observed with the Climenhaga Observatory 0.5m telescope. Like on HJD 245 1052, we again find that the difference in brightness between V773 Tau and CW Tau remained constant. If we then average all data-points before HJD 245 1057.885, and all measurements after that time, we find that

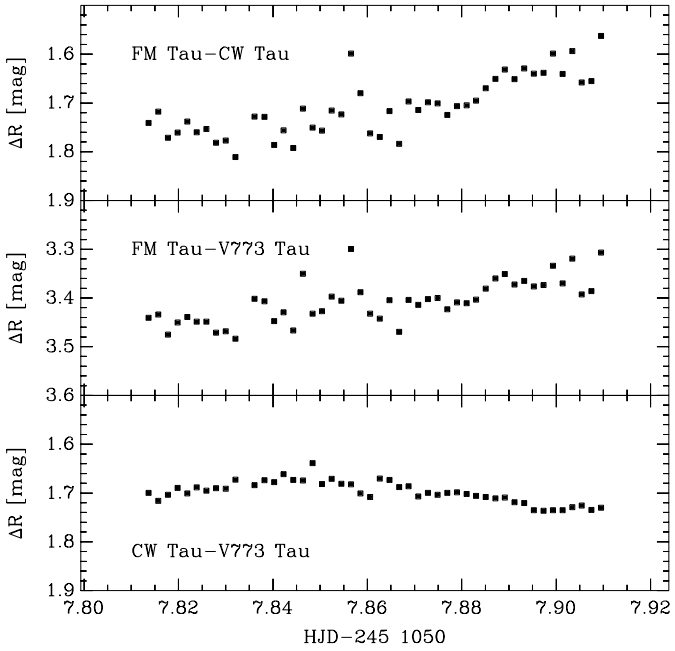

Fig. 10. Same as Fig. 7 but for HJD 245 1057. The scatter of the points in the upper two panels must be due to FM Tau. If we average all data-points before HJD 245 1057.885, and all data-points after that, we find that the brightness of FM Tau increased by 0.085 ± 0.021 mag in the R band. Interestingly, the increase of the equivalent width in CW Tau observed in this night (Fig. 11 and Fig. 12) thus does not seem to have resulted a brightening of it.

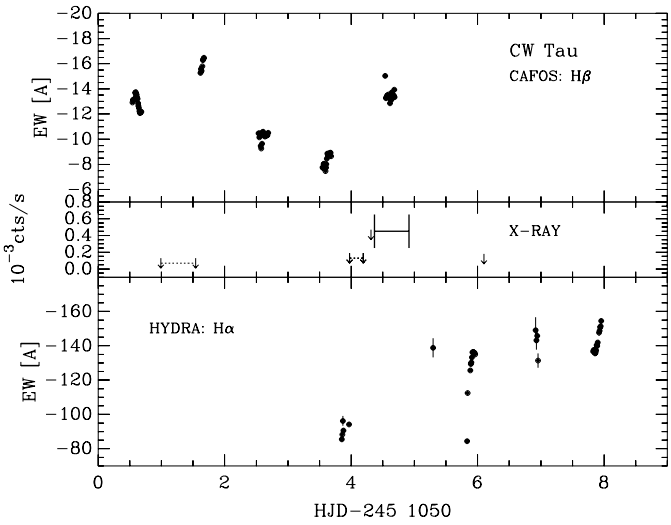

Fig. 11. Same as Fig. 6 but for CW Tau. CW Tau has only once been detected with ROSAT. This detection is shown as a full line with the errors indicated at the beginning and at the end of the observations. The upper limits are again indicated as an arrow pointing downwards. CW Tau is apparently a highly active object and exhibits large night-to-night variations of the equivalent widths of the Balmer lines.

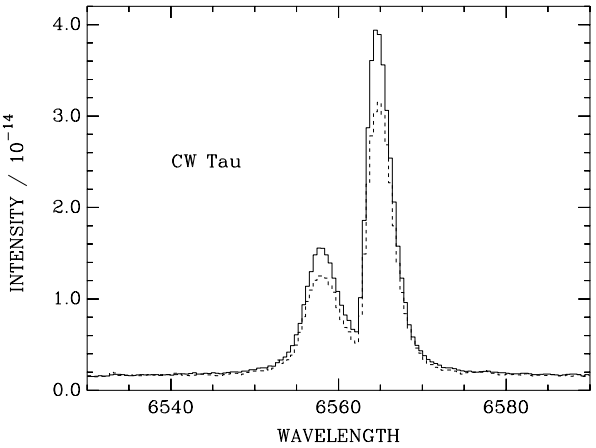

Fig. 12. Hα line-profiles of CW Tau. As can be seen in Fig. 11, during the last night, the Hα line becomes stronger as the night progresses. The dashed line is the spectrum at the beginning of the observations (HJD 245 1057.830), and the full line the spectrum which was taken three hours later. (HJD 245 1057.955). We find that while the equivalent width changed, the structure of the P-Cygni profile remained constant.

the brightness of FM Tau increased by 0.085 ± 0.021 mag in the R-band. While the observed increase of flux of the Hα line is clearly flare-like, the increase of the continuum brightness is slow and steady (Fig. 10).

3.5. The cTTS CW Tau

CW Tau is a known jet source (Gómez de Castro 1993; Hirth et al. 1994) that has been studied extensively. With ROSAT we detected CW Tau in only one of the RORs. It is thus not possible to derive anything about the X-ray variability of this object. Fig. 11 shows the equivalent width of Hβ as observed with CAFOS, the equivalent width of Hα as observed with HYDRA, and the X-ray data from ROSAT. In the optical, CW Tau exhibits a wealth of activity, and the equivalent width changes from night to night. CW Tau was not detected by ROSAT between HJD 245 1053.976 and HJD 245 1054.193; but, if it would have been as bright as on HJD 245 1054.5 between HJD 245 1054.369 and HJD 245 1054.913, it would have been detected.

It is interesting to note that CW Tau was detected by ROSAT on a day when its equivalent width of Hβ was particularly large. However, CW Tau was not detected on HJD 245 1051, although the equivalent width of Hβ shortly before and after the ROSAT observations was high. However, we cannot be sure what the equivalent width at the time of the ROSAT observation actually was, as significant changes of the equivalent width during a night were also observed in CW Tau. An increase of the Hα-strength was observed during the last night of HYDRA observations. Fig. 12 shows the profile of Hα at the beginning of the observations on that night (HJD 245 1057.830) and three hours later at the end of the night (J.D. 245 1057.954). Although the line profile is clearly resolved as a P-Cygni profile in the HYDRA spectra, we do not see any changes of the line-profiles but only changes of the equivalent width. Interestingly, the increase of the equivalent width in CW Tau did not result in a brightening of the star (Fig. 10).

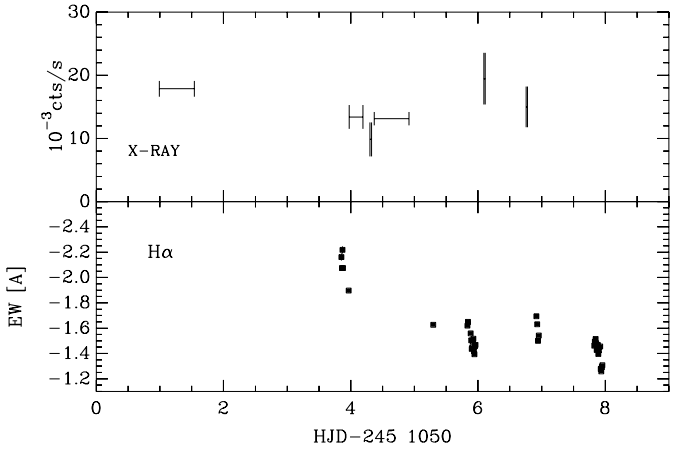

Fig. 13. The lower panel shows the equivalent width of Hα for HBC 366, and the upper panel the ROSAT count rate. The source has been detected in each ROR.

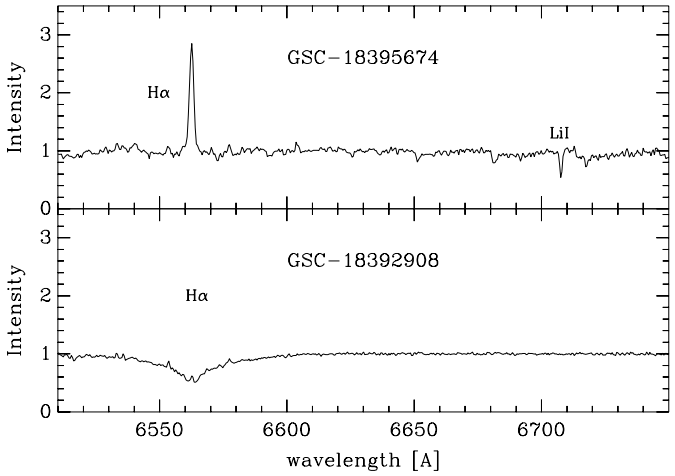

Fig. 14. Spectra of GSC-1839-5674, and GSC-1839-2008 taken with HYDRA. The strong LiI 6707 line in GSC-1839-5674 indicates its pre-main sequence nature. GSC-1839-2008 apparently is an A-star. Thus, the LiI-test does not work in this case.

3.6. The second brightest X-ray source: HBC 366

HBC 366 is a wTTS which is quite bright in X-rays (see Table 2). Due to the large brightness, ROSAT detected the source in every ROR. Fig. 13 shows the X-ray flux together with the equivalent width of Hα. The ROSAT data on HJD 245 1054 and 245 1056 partly overlaps the Hα monitoring; and, on 245 1057, the good X-ray data was taken shortly before the optical data. On HJD 245 1056, the X-ray flux was higher, and the equivalent width was lower than during the other nights. However, the error bars of the X-ray measurements still overlap with the two other nights. Although we detected significant night-to-night variations of the X-ray brightness, the activity of this star seems to be quite low. The equivalent width of Hα is also quite stable. Only on HJD 245 1054 was Hα much stronger than on the other nights.

3.7. A newly discovered weak-line T Tauri star

An interesting by-product of our observations was the detection of a new pre-main sequence star, GSC-1839-5674. The equivalent width of of the LiI 6707 Å line is 0.582 ± 0.050 and we derive a spectral type of K5, indicating that the object is a pre-main sequence star. GSC-1839-5674 is also remarkably bright in X-rays and has been detected in all but one RORs with ROSAT (see Table 2). As can be seen in Fig. 14, Hα is an emission line. Since the equivalent width is -4.5 Å, GSC-1839-5674 is a wTTS.

We also observed GSC-1839-2008. Since GSC-1839-2008 is apparently an A-star we do not expect to see the LiI 6707 line anyway. We are thus unable to tell, whether this star is pre-main sequence or not (Fig. 14). The X-ray variability of GSC-1839-2008 is quite low (Table 2).

4. Discussion

4.1. General properties of the X-ray emission

For the T Tauri stars studied, we often observed relatively large night-to-night variations of the X-ray brightness. For example, on one occasion, the X-ray flux of the cTTS FM Tau changed by a factor of four from one night to the next. Large night-to-night variations were also detected for the wTTS binary V773 Tau and the cTTS CW Tau. Compared to these stars, the wTTSs GSC-1839-5674 and HBC 366 are less active, although significant night-to-night variations were detected. Only the data for V773 Tau was abundant enough to draw any conclusions about the relation between the X-ray brightness and optical line emission. In this object, we find a weak correlation between the Hα equivalent width and the X-ray brightness. Because V773 Tau is a wTTS, this observation implies a relation between the coronal and chromospheric emission.

What could be the cause of such a relation? Solar flares produce both chromospheric lines and X-ray emission. Simultaneous optical and X-ray observations of a solar flare show that the light curves of Hβ and soft X-rays (0.25-4.0 keV) are almost identical, implying that Balmer-lines are probably produced during a flare by the soft X-ray radiation (Johns-Krull et al. 1997). The same close relation between X-ray emission and Hα is also observed in flares on RS CVn and BY Dra stars (Doyle et al. 1988). Thus, if the Hα-line and X-ray emission were just a superposition of solar-like flares, we would expect a much higher correlation than we observed.

As shown by Hempelmann et al. (1997) for RS CVn binary stars, the X-ray light curve can be reproduced if it is assumed that the extended coronal X-ray emission regions are located above photospheric regions where the spots are. Additionally, Doppler image reconstructions of the distribution of the spots and measurements of the strength of Hα for the RS CVn star DM UMa by Hatzes (1995) show that the strongest chromospheric emission comes from regions above the spots. Such a situation would naturally also lead to a weak but not necessarily one-to-one correlation between chromospheric Hα and the coronal X-ray emission. The idea that V773 Tau is a pre-main

sequence analogue of an RS CVn object would thus explain our observations. So, we suggest that the X-rays in this object are generated in a hot corona which is situated above active regions with spots. Future Doppler image reconstructions or at least high-precision RV-measurements combined with X-ray observations of this object may prove this idea.

The data for the cTTSs CW Tau and FM Tau are certainly not good enough to do the same analysis.

The fact that the X-ray emission and the equivalent width of Hα in V773 Tau remained unchanged while large variations of the flux density in the radio regime were observed clearly indicates that the emitting regions are different (Fig. 2). This result is in excellent agreement with the observation by Feigelson et al. (1994). The observation thus imply that the radio-emission is gyrosynchrotron radiation that arises presumably from a large, extended region. The X-ray radiation seems to be the emission of a hot, extended corona but this region has to be different from the radio-emitting region.

4.2. The detection of a flare in Hα in a cTTS

In previous observations, flares in cTTSs were always detected in Hβ and the higher Balmer lines but not in Hα (Guenther & Emerson 1997; Guenther & Ball 1999). These authors argued that this was due to high optical depth in Hα. With our new observation, we conclude instead that Hα can sometimes be sufficiently optically thin in some cTTSs to allow observations of Hα flares. On one occasion the increase in flux of the Hα line of FM Tau is stronger in the blue wing than in the red. In stellar spectra, coronal mass-ejections show up as blue shifted components. Coronal mass-ejections are often accompanied by flares, and have also been observed in wTTSs (Guenther & Ball 1999). However, for a coronal mass-ejection the velocity of the matter has to be larger than the escape velocity of the star, which is about 300 $\mathrm{km\,s^{-1}}$ for a T Tauri star. Since the line of sight velocity of the event observed in FM Tau is much smaller than that, we cannot be sure whether this matter actually left the star but we can conclude that matter moved away from the star like in a coronal mass-ejection. It is interesting to note that the Hα flare did result in brightening of the star, indicating that continuum flares, and emission line flares have the same origin. Unfortunately ROSAT did not observe the field at the time of the Hα flares, and so it is not yet clear, whether the events are accompanied by X-ray flare events.

4.3. The detection of a flare-like event in a cTTS

Altough numerous large white-light flares ($\Delta U > 0.2mag$) were observed in wTTSs (Gahm 1990; Gahm et al. 1995, the situation is more complex in the case of the cTTSs. First of all, most of the events show a slow instead of a rapid increase of the broad-band colours (Gahm 1990). Secondly, the events on cTTSs that do show flare-like variations (e.g. Kiliachov & Shevchenko 1976) are significantly redder than typical flares on other stars (Gullbring 1994; Gullbring et al. 1996a). Events on cTTSs are thus often interpreted as due to variations of the extinction or variations of the veiling continuum instead of flares (Gahm 1990; Gullbring et al. 1996a). This conclusion is further supported by simultaneous spectroscopic and photometric monitoring of two cTTSs and three wTTSs by Gahm et al. (1995), and by the monitoring of BP Tau by Gullbring et al. 1996a. On the other hand, with time-resolved spectroscopy of cTTSs, events are seen which show a flare-like increase and decrease of the emission lines. Additionally, the lines that are enhanced are the same as in flares on the sun, and on flare-stars. Such an event has also been observed on the *cTTS* FM Tau (Guenther & Ball 1999). It is thus interesting to note that we observed a flare in Hα in FM Tau simultaneously with a slow increase of the continuum brightness. These observations certainly leave room for interpretation. The first possibility is that the Hα event was in fact a flare, and the slow continuum increase at the same time just coincidental. The second possibility would be that the two events are related, implying that also slow events have something to do with flares. We also observed an event with rapid increase of the $H\alpha$ equivalent width and slow decrease in the continuum during another night also on FM Tau.

4.4. The X-ray event in V773 Tau

In V773 Tau, we observed an event in which the X-ray flux increased for about 8 hours and then decreased back to the pre-event level in 5 hours. The total duration of the event is about one-sixth of the photometric period of the spectroscopic binary, which has been interpreted as the rotation period of both stars (Rydgren & Vrba 1983; Welty 1995). It is thus not very likely that the X-ray light curve was caused by an active region rotating in and out of view. The light-curve does not look like a flare either, or what is usually assumed to be a flare.

However, the X-ray light-curves of the so-called "long-duration events" on the sun occasionally look like Fig. 3. The rise time of these events is often many hours, and the decay time is often about as long as the rise time. Such events have been observed on the sun (e.g. Lantos et al. 1981; Kreplin et al. 1985) and on active stars (e.g. Schmitt 1994). With ASCA Tsuboi et al. (1998) observed a strong flare in V773 Tau that showed a very high, and possibly variable absorption column density. Since ROSAT observes at much lower energies than ASCA, such a flare in which the column density declines from very high values to lower values might actually look like Fig. 3 if observed with ROSAT. Thus, the shape of the curve by no means rules out a flare. Since long-duration events are often accompanied by coronal mass-ejections, these events are important for mass loss by the stars. Until now, events with a slow rise time of the optical line and continuum emission have usually been interpreted as changes in the accretion rate, not as flares (Gahm 1990; Gahm et al. 1995; Guenther & Ball 1999). This interpretation seemed reasonable because they were usually observed in cTTSs. The possible detection of a long-duration event on a wTTS in X-rays may force us to rethink the interpretation of similar events in cTTSs as well.

4.5. The X-ray event in CW Tau

The variability observed in CW Tau is certainly different from normal flare activity. For example, we observed a slow increase of the Hα strength over three hours, during which the star did not become notably brighter. Although we cannot exclude a slow event, a change of the accretion rate seems more plausible. The fact that only the equivalent width went up, and the P-Cygni absorption feature remained unchanged indicates that the structure of the outflowing wind remained the same. Since the emission is probably related more to the inflow, the fact that the whole line-profile is unchanged may indicate that also the structure of the funnel flow did not change. We thus interpret the observation by a change of the accretion rate in which the structure of the flow pattern remained unchanged.

5. Conclusions

We have analysed a time-series of X-ray observations, optical spectroscopy, and optical photometry of a sample of cTTSs and wTTSs in the dark cloud Barnard 209, which is part of the Taurus-Auriga star-forming region. Significant night-to-night variations of the X-ray emission have been detected in all objects, if they were detected by ROSAT at all. Relatively large night-to-night variations were detected in the cTTSs FM Tau and CW Tau and in the wTTSs V773 Tau. Night-to-night variations in the wTTSs GSC-1839-5674 and HBC 366, though detected, were of much smaller amplitude.

From observations taken simultaneously, we find that there is some correlation between the strength of Hα and the X-ray brightness in V773 Tau, but the weakness of the correlation implies that the X-ray emission is probably not due to a superposition of flares. On the other hand, the presence of some correlation indicates that the X-ray emitting regions and the regions in which Hα is formed are related. Since V773 Tau resembles an RS CVn binary star in many respects, we interpret this correlation in the same way as for these stars, namely that regions of strong chromospheric and coronal emission tend to be located above the stellar spots. Thus, we conclude that the X-ray emission in V773 Tau is presumably generated in the same way as in RS CVn stars, i.e., in a hot corona.

In this campaign, we also detected flares on cTTSs in Hα and a flare-like event in the continuum. These observations further strengthen that the flares on cTTSs can be observed in the optical regime. Since the Hα flare did result in a small brightening of the star, we conclude that continuum flares and emission line flares occur simultaneously. However, the attitude problems of ROSAT did not allow scheduling of the observations as originally planned, and so ROSAT did not observe the field at the times of the optical flares.

An interesting X-ray event was observed in V773 Tau. During this event the flux increased for about 8 hours and then decreased back to the pre-event level in 5 hours. We interpret this as a long-duration event similar to those seen on the sun or other active stars. Such events can be accompanied by coronal mass-ejection. The detection of such an event re-enforces the identification of the wTTS V773 Tau as a pre-main sequence analogue of an RS CVn star. The event in V773 Tau also resembles the broad-band variations in cTTSs usually attributed to variations in the accretion rate. This suggests a need for caution about the interpretation of photometric variability in cTTSs.

A by-product of the observations was the discovery of a new pre-main sequence star, the wTTS GSC-1839-5674.

Acknowledgements. We are grateful to the support group of ROSAT for making the observations possible and helping us with the data reduction. ROSAT is supported by the german government (DLR/BMB+F) and the Max-Planck-Society. We would also like to thank the staff of the WIYN telescope at Kitt Peak for all their help and assistance. Many thanks go also to the staff of the Calar Alto Observatory for their help and assistance. We are grateful to the referee, Dr. Gösta Gahm, for very valuable comments that contributed to improve this work. We acknowledge the use of IRAF, MIDAS, STARLINK and AIPS software for preparing the observations and for analysing the data.

References

Alcalá J.M., Covino E., Franchini M., et al., 1993, A&A 272, 225
Appenzeller I., Mundt R., 1989, A&AR 1, 291
Canuto V.M., Levine J.S., Augustsson T.R., Imhoff C.L., 1982, Nat 296, 816
Canuto V.M., Levine J.S., Augustsson T.R., Imhoff C.L., Giampapa M.S., 1983, Nat 305, 281
Crosa L., Szkody P., Stokes G., Swank J., Wallerstein G., 1981, ApJ 247, 984
Doyle J.G., Butler C.J., Callman P.J., et al., 1988, A&A 191, 79
Dutrey A., Guilloteau S., Duvert G., et al., 1996, A&A 309, 493
Feigelson E.D., Casanova S., Montmerle T., Guibert J., 1993, ApJ 416, 623
Feigelson E.D., Welty A.D., Imhoff C.L., et al., 1994, ApJ 432, 373
Gahm G.F., 1990, In: Mirzoyan L.V., Pettersen, Tsvestkov M.K. (eds.) Proc. IAU Symp 137, Flare Stars in Star Clusters, Associations and the Solar Vicinity. p. 193
Gahm G.F., Lodén K., Gullbring E., Hartstein D., 1995, A&A 301, 89
Ghez A.M., Weinberger A.J., Neugebauer G., Matthews K., McCarthy Jr. D.W., 1995, AJ 110, 753
Glassgold A.E., Najita J., Igea J., 1997a, ApJ 480, 344
Glassgold A.E., Najita J., Igea J., 1997b, ApJ 485, 920
Gómez de Castro A.I., 1993, ApJ 412, L43
Güdel M., 1997, ApJ 480, L121
Güdel M., Guinan E.F., Skinner S.L., 1997, ApJ 483, 947
Guenther E.W., Emerson J.P., 1997, A&A 321, 803
Guenther E.W., Lehmann H., Emerson J.P., Staude J., 1999, A&A 314, 768
Guenther E.W., Ball M., 1999, A&A 347, 508
Gullbring E., 1994, A&A 287, 131
Gullbring E., Barwing H., Chen P.S., Gahm G.F., Bao M.X., 1996a, A&A 307, 791
Gullbring E., Petrov P.P., Ilyin I., et al., 1996b, A&A 314, 835
Gullbring E., Barwig H., Schmitt J.H.M.M., 1997, A&A 324, 155
Hempelmann A., Hatzes A.P., Kürster M., Patkós L., 1997, A&A 317, 125
Hatzes A., 1995, AJ 109, 350
Hessman F.V., Guenther E.W., 1997, A&A 321, 497
Hirth G.A., Mundt R., Solf J., 1994, A&A 285, 929
Igea J., Glassgold A.E., 1999, ApJ 518, 848
Johns-Krull Ch.M., Hawley S.L., Basri G., Valenti J.A., 1997, ApJS 487, 896

Kiliachov N.N., Shevchenko V.S., 1976, SvA Lett. 2, 193
Kreplin R.W., Doschek G.A., Feldman U., Sheeley Jr. N.R., Seely J.F., 1985, ApJ 292, 309
Kutner M.L., Rydgren A.E., Vrba F.J., 1986, AJ 92, 895
Lamzin S.A., Bisnovatyi-Kogan G.S., Errico L., et al., 1996, A&A 306, 877
Lantos P., Kerdraon A., Rapley G.G., Bentley R.D., 1981, A&A 101, 33
Muzerolle J., Hartmann L., Calvet N., 1998, AJ 116, 2965
Neuhäuser R., Sterzik M.F., Schmitt J.H.M.M., Wichmann R., Krautter J., 1995, A&A 297, 391
Neuhäuser R., 1997, Sci 276, 1363
O'Neal D., Feigelson E.D., Mathieu R.D., Myers P.C., 1990, AJ 100, 1610
Paerels F., Heise J., Teeseling A., 1994, ApJ 426, 313
Phillips R.B., Lonsdale C.J., Feigelson E.D., 1991, ApJ 382, 261
Phillips R.B., Lonsdale C.J., Feigelson E.D., Deeney B.D., 1996, AJ 111, 918
Preibisch Th., Zinnecker H., Schmitt J.H.M.M., 1993, A&A 279, L33
Preibisch Th., Neuhäuser R., Alcalá J.M., 1995, A&A 304, L13
Robb R.M., Greimel R., Ouellette J., 1997, IBVS No. 4504
Rydgren A.E., Vrba F.J., 1983, ApJ 267, 191
Skinner S.L., Güdel M., Koyama K., Yamauchi S., 1997, ApJ 486, 886
Schmitt J.H.M.M., 1994, ApJS 90, 735
Tsuboi Y., Koyama K., Murakami H., et al., 1998, ApJ 503, 894
Welty A.D., 1995, AJ 110, 776
White S.M., Pallavicini R., Kundu M.R., 1992, A&A 259, 149
Zimmermann H.U., Becker W., Izzo C., et al., 1995, EXSAS Handbook. Garching